ScienceDirect

Journal of Rare Earths

Supports *open access*

5.8	3.712
CiteScore	Impact Factor

Submit your article | Guide for authors

Menu Search in this journal

About the journal

Aims and scope | Editorial board | Abstracting and indexing

Editor-in-Chief

Chun-Hua Yan
Peking University, Beijing, China
Email this editor

Associate Editors-in-Chief

J-C Bünzli
ETH Zurich, Zurich, Switzerland

Hongjie Zhang
Changchun Institute of Applied Chemistry Chinese Academy of Sciences, Changchun, China

Executive Associate Editor-in-chief

Xiaowei Huang
General Research Institute for Nonferrous Metals, Beijing, China

FEEDBACK

Chairman

Chunlong Li
The Chinese Society of Rare Earths, Beijing, China

Vice-Chairman

Jingkao Niu
The Chinese Society of Rare Earths, Beijing, China

Advisors

Wenjiang Ding
Shanghai Jiao Tong University School of Materials Science and Engineering, China

Yong Gan
Chinese Academy of Engineering, China

Song Gao
Peking University, China

Chunhui Huang
Peking University, China

Lemin Li
Peking University, China

Wei Li
Central Iron and Steel Research Institute Group, China

Yongxiu Li
Nanchang University, China

Jiazuan Ni
The Chinese Society of Rare Earths, China

Bao-Gen Shen
Chinese Academy of Sciences, China

Hailing Tu
General Research Institute for Nonferrous Metals, China

FEEDBACK

Zhenxi Wang
Beijing Zhongke SanHuan Hi-tech Co. Ltd., China

Yingchang Yang
Peking University, China

Guocheng Zhang
General Research Institute for Nonferrous Metals, China

Members of Editorial Board

Ana de Bettencourt-Dias
University of Nevada Reno, Nevada, United States of America

Koen Binnemans
KU Leuven Department of Chemistry, Belgium

John A. Capobianco
Concordia University John Molson School of Business, Quebec, Canada

Luis D. Carlos
University of Aveiro, Portugal

Chi-Ming Che
The University of Hong Kong State Key Laboratory of Synthetic Chemistry, Hong Kong

Jun Chen
Nankai University, China

Xueyuan Chen
Chinese Academy of Sciences Fujian Institute of Research on the Structure of Matter, China

Yungui Chen
Sichuan University, Sichuan, China

Dante Gatteschi
University of Florence, Italy

Zhengping Hao
Research Centre for Eco-Environmental Sciences Chinese Academy of Sciences, China

Jorma Holsa

FEEDBACK

University of Turku, Finland

Boping Hu
Beijing Zhongke SanHuan Hi-tech Co. Ltd., China

Nobuhito Imanaka
Osaka University, Japan

Jianzhuang Jiang
University of Science and Technology Beijing, China

Lijun Jiang
General Research Institute for Nonferrous Metals, China

Tao Jiang
Central South University, China

Dayong Jin
University of Technology Sydney, Australia

Xingguo Li
Peking University, China

Chunfa Liao
JiangXi University of Science and Technology, China

Jun Lin
Changchun Institute of Applied Chemistry Chinese Academy of Sciences, China

Stefan Lis
Adam Mickiewicz University, Poland

Ru-Shi Liu
National Taiwan University Chemistry Department, Taiwan

Andries Meijerink
Utrecht University Debye Institute for Nanomaterial(s) Science, Netherlands

Jian Meng
Changchun Institute of Applied Chemistry Chinese Academy of Sciences, China

Xujun Mi

FEEDBACK

General Research Institute for Nonferrous Metals, China

Ritsuro Miyawaki
National Museum of Nature and Science Zoology, Japan

Masato Murakami
Shibaura Institute of Technology College of Engineering Department of Materials Science and Engineering, Japan

Zuoren Nie
Beijing University of Technology, China

Xiaogang Qu
Changchun Institute of Applied Chemistry Chinese Academy of Sciences, China

Guohao Ren
Shanghai Institute of Ceramics Chinese Academy of Sciences, China

Huiping Ren
Inner Mongolia University of Science and Technology, China

Wieslaw Strek
Institute of Low Temperature and Structure Research Polish Academy of Sciences, Poland

Cheng-Yong Su
Sun Yat-sen University School of Chemistry, China

Jirong Sun
Chinese Academy of Sciences Institute of Physics, China

Ling-Dong Sun
Peking University, China

Yu Tang
Lanzhou University, China

Mingliang Tong
Sun Yat-sen University School of Chemistry, China

Alessandro Trovarelli
University of Udine Department of Chemistry Physics and Environment, Italy

FEEDBACK

Ligen Wang
General Research Institute for Nonferrous Metals, China

Xiao-jun Wang
Georgia Southern University Department of Physics and Astronomy, Georgia, United States of America

Xianran Xing
University of Science and Technology Beijing, China

Dongfeng Xue
Shandong University, State Key Laboratory of Crystal Materials, Shandong, China

Aru Yan
Ningbo Institute of Industrial Technology Chinese Academy of Sciences, China

Xiaoda Yang
Peking University School of Pharmaceutical Sciences, China

Zhanfeng Yang
Baotou Research Institute of Rare Earths, China

Anwen Zhang
The Chinese Society of Rare Earths, China

Hong Zhang
University of Amsterdam, Netherlands

Dongliang Zhao
Central Iron and Steel Research Institute Group, China

Zhen Zhao
China University of Petroleum Beijing, China

Zhiping Zheng
The University of Arizona, Arizona, United States of America

Weidong Zhuang
General Research Institute for Nonferrous Metals, China

All members of the Editorial Board have identified their affiliated institutions or organizations, along with the corresponding country or geographic region. Elsevier

FEEDBACK

remains neutral with regard to any jurisdictional claims.

ISSN: 1002-0721

Copyright © 2022 The Chinese Society of Rare Earths. Published by Elsevier B.V. All rights reserved

Copyright © 2022 Elsevier B.V. or its licensors or contributors.
ScienceDirect ® is a registered trademark of Elsevier B.V.

Journal of Rare Earths 37 (2019) 1320–1325

Contents lists available at ScienceDirect

Journal of Rare Earths

journal homepage: http://www.journals.elsevier.com/journal-of-rare-earths

Selective microwave absorption in Nd^{3+} substituted barium ferrite composites☆

Wahyu Widanarto [a, *], Siti Khaeriyah [a], Sib Krishna Ghoshal [b], Candra Kurniawan [c], Mukhtar Effendi [a], Wahyu Tri Cahyanto [a]

[a] Department of Physics, FMIPA, Universitas JenderalSoedirman, Jl. dr. Soeparno 61, Purwokerto, 53123, Indonesia
[b] Department of Physicsand Laser Centre, AMORG, Faculty of Science, Universiti Teknologi Malaysia, Johor Bahru, Skudai, 81310, Malaysia
[c] Research Center for Physics, Indonesian Institute of Sciences (LIPI), Puspiptek Office Area, South Tangerang, Banten, 15314, Indonesia

ARTICLE INFO

Article history:
Received 22 September 2018
Received in revised form
18 January 2019
Accepted 22 January 2019
Available online 28 June 2019

Keywords:
Neodymium doping
Barium ferrite composites
Magnetic properties
Porosity
MW reflection loss
Rare earths

ABSTRACT

Microwave (MW) frequency based wireless communications and electronic devices became prospective due to several ramifications. To meet this need, a series of neodymium ions (Nd^{3+}) substituted barium ferrite composites with composition (20)BaO:(80−x)Fe_2O_3:(x)Nd_2O_3 ($0 \leq x \leq 3$ mol%) was prepared at 1100 °C using solid-state reaction method. We evaluated the effect of various Nd^{3+} ions contents on the surface morphology, structure, and magnetic properties of the as-synthesized barium ferrite composites. Meanwhile, microwave reflection loss, complex permittivity and permeability were determined using the transmission/reflection line method in the X-band (8−12 GHz). SEM image of the composites shows that the surface morphology consists of rough and porous microstructures. XRD patterns of the un-doped composites reveal the existence of $BaFe_{12}O_{19}$ (hexagonal) and $Fe_{21.333}O_{32}$ (tetragonal) crystalline phases. Furthermore, a new hexagonal crystalline phase of $Ba_6Nd_2Fe_4O_{15}$ with the crystallite sizes between 15 and 67 nm is observed due to Nd^{3+} ions substitution in the composite. The saturation magnetization of the composite containing 2 mol% of Nd^{3+} does not exhibit any significant alteration compared to the one devoid of Nd^{3+}. The complex relative permitivity and permeability of the achieved composites enriched in $Ba_6Nd_2Fe_4O_{15}$ and $BaFe_2O_4$ phases disclose significant MW frequency dependence. The composites also display selective MW absorption in the X-band which could be useful for diverse applications.
© 2019 Chinese Society of Rare Earths. Published by Elsevier B.V. All rights reserved.

1. Introduction

In recent times, wireless communications and electronic devices based on the microwave (MW) frequency in the range of 8−12 GHz (X-band) received focused attention, wherein dedicated efforts have been made to achieve the emission of such frequencies from a transmitter and radar. Materials required for such purposes must be capable in attenuating and dissipating the excess amount of electromagnetic energy in the form of thermal energy via magnetic and dielectric loss mechanisms.[1] Thus, novel magnetic materials (ferrites based) appropriate for absorbing the electromagnetic energy(MW) have continually been explored.[2–10] In this regard, barium hexaferrite (BHF) owing to its extremely high uniaxial magnetic anisotropy showed an emergent MW absorbing material.[3–5,11,12] Thus, it became essential to optimize the MW absorption capacity of these ferrites in the X-band (8−12 GHz).

It was demonstrated that the natural resonance-frequencies, saturation magnetization, permeability, permittivity and magnetic field anisotropy of such ferrites could be altered by incorporating divalent or trivalent ions into the crystalline structures.[13–15] Consequently, the effects of electromagnetic interferences in these ferrites could be improved. Meanwhile, outstanding relaxation attributes of rare earth ions (REIs) as dopants inside the BHF have also been exploited to alterits magnetic and MW absorption characteristics.[3,13,16–19] Besides, BHF doped with REIs revealed weak coercive field (H_c) and low saturation magnetization (M_s) which could be useful for the enhancement of MW absorption capacity.[6,13,20,21] Inspired by these innovations, we took an attempt to diminish the values of H_c and M_s of the prepared barium ferrite composites (BFCs), there by enhancing the selective absorption of MW frequencies.

☆ **Foundation item:** Project supported by the PBK 2021/UN23.14/PN/2018 (Indonesia) and GUP/RU/KPT 18H68/17H19 (UTM, Malaysia).
* Corresponding author.
E-mail address: wahyu.widanarto@unsoed.ac.id (W. Widanarto).

https://doi.org/10.1016/j.jre.2019.01.008
1002-0721/© 2019 Chinese Society of Rare Earths. Published by Elsevier B.V. All rights reserved.

This communication reports the production and characterizations of new BFCs (hereafter referred as NdBFCs) wherein the Fe^{3+} ions in pure BHF were replaced by Nd^{3+} ions (at various concentrations). Trivalent Nd^{3+} due to their compatible hexagonal lattice structure and excellent relaxational attributes were selected as doping agents (so-called substituent ions). Two types of composites (undoped and doped with Nd^{3+} ions) were synthesized via tailored solid–state reaction method. As-prepared composites were characterized using different analytical tools to determine the influence of Nd^{3+} ions on the microstructures, surface morphologies, magnetic characteristics, and MW reflection loss in the X–band. Achieved $Ba_6Nd_2Fe_4O_{15}$ and $BaFe_2O_4$ phases of the proposed BFCs were shown to be beneficial for sundry applications.

2. Experimental

Few BFCs (one without and three with Nd^{3+} ions doping) with the composition of $(20)BaO:(80-x)Fe_2O_3:(x)Nd_2O_3$, where $0 \leq x \leq 3$ mol% were prepared using modified solid-state reaction strategy. High purity powders (analytical grade) of $BaCO_3$ (Merck, 99%), Nd_2O_3 (Sigma Aldrich, 99%) and Fe_2O_3 (Sigma Aldrich, 99%) were used as preparatory materials to synthesize such BFCs. Furthermore, the $BaCO_3$ powder was calcined at 300 °C for an hour to remove the existed carbon element. Later, BaO powder was mixed gradually with Fe_2O_3 via annealing and sintering processes. Afterward, the Nd_2O_3 powder was added to the mixture and thoroughly mixed using a magnetic stirrer at the revolution speed of 700 r/min (rotation per minute) for 2 h. Polyvinyl alcohol (PVA) was mixed and stirred continually until a sol was achieved. After that, the composite powder was compacted to produce pellets with the respective thickness and diameter of 1 mm and 1 cm.[13] Besides, some pellets of rectangular shape with a dimension of 2.5 cm × 1.5 cm × 0.2 cm were obtained for additional characterizations. These pellets were further annealed at 800 °C for 1 h and sintered at 1100 °C for 5 h[22] before being cooled down naturally to room temperature. The achieved pellets were named as NdBF0, NdBF1, NdBF2 and NdBF3 based on their corresponding Nd^{3+} ions content of 0 mol%, 1 mol%, 2 mol% and 3 mol%. Finally, the prepared composites were characterized at room temperature using different analytical techniques to determine the feasibility of achieving their selective MW absorption effectiveness in the X-band.

A scanning electron microscope (SEM, Hitachi SU 3500) equipped with energy dispersive X-ray (EDX, Horiba) was utilized to determine the surface morphologies, microstructures and elemental compositions of the synthesized NdBFCs.[13,21,23] The presence of crystalline phases in the studied NdBFCs was verified using X-ray diffraction measurement (XRD, SmartLab 3 kW) equipped with Cu Kα radiation of wavelength (λ) 0.1541874 nm. A vibrating sample magnetometer (VSM, Oxford 1.2H) was employed to examine the magnetic behavior of the studied composites. The scattering (S) parameters of the proposed composites were measured using a Vector network analyzer (VNA, Advantest R3770) operated in the frequency range of 8–12 GHz. Additionally, the transmission/reflection line method was exploited to determine the MW reflection loss (R_L), the complex relative permittivity and permeability.

3. Results and discussion

3.1. Surface morphology and elemental traces

Fig. 1 displays the SEM images of all synthesized composites, wherein the surface morphology consisted of porous microstructures with roughness. Overall, the composites surface morphology and the distribution of particles size were influenced due to the Nd^{3+} ions substitution into the crystalline lattices. At higher Nd^{3+} concentrations, the microstructure manifested two phases including the hexagonal grains of barium ferrite (dark color) and Nd-rich (bright color) regions. The microstructure of NdBF2 was

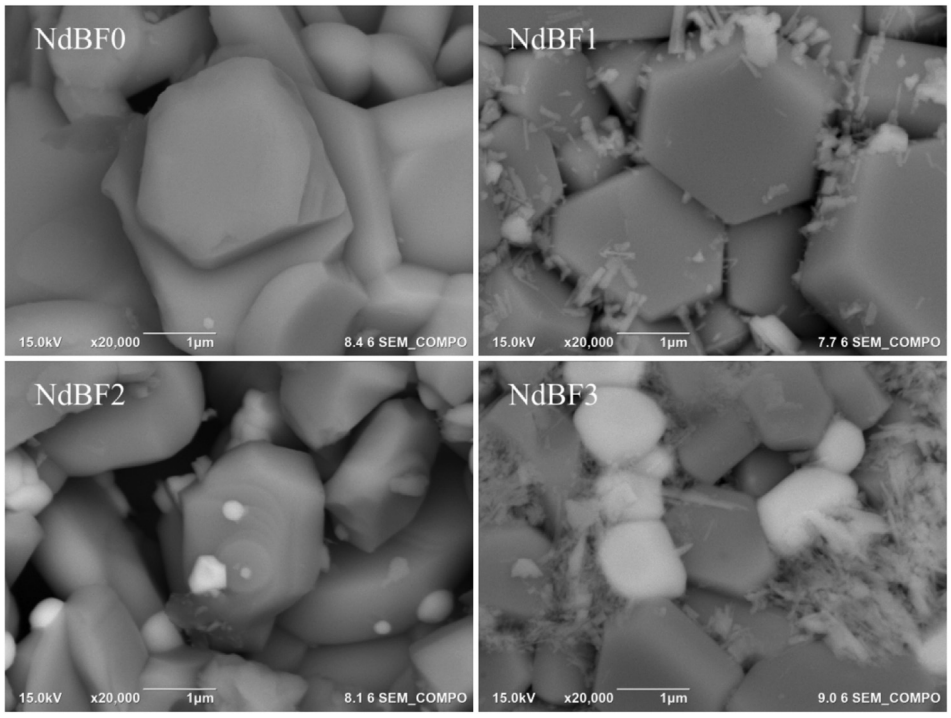

Fig. 1. SEM micrographs of the as-synthesized NdBFCs.

more porous than the other samples. The mean grain size BFCs was shrunk from 2.5 to 1 μm with the increase in the Nd^{3+} ions content from 0 to 3 mol% accompanied by porosity enhancement. This enrichment in the porosity led to an improvement in the magnetic characteristics and MW-reflection loss.[21] Fig. 2 depicts the EDX spectra of all BFCs, confirming the appropriate elemental traces of O, Fe, Ba and Nd where in the inclusion of Nd in the composite caused an adjustment in the level of other elements (table in the inset). Sample NdBF2 revealed the minimum traces of Nd (0.1 at%), and NdBF3 exhibited the highest level of Nd (0.3 at%).

3.2. Crystalline structure and sizes

Fig. 3 illustrates the XRD patterns of the synthesized composites which comprised of several sharp peaks characteristics of different crystalline lattices. For the sample without Nd^{3+} substitution (NdBF0), all the observed peaks were assigned to the dominant hexagonal crystalline structure of $BaFe_{12}O_{19}$ which matched with the ICDD number 00-027-1029 with crystallographic parameters of $a = b = 0.5892$ nm, $c = 2.3198$ nm, $\alpha = \beta = 90°$ and $\gamma = 120°$. However, the peak that appeared at 28.36° was allocated to the tetragonal crystal structure of $Fe_{21.333}O_{32}$ which was tallied with the ICDD numbers 01-076-1470. Furthermore, substitution of Fe^{3+} by Nd^{3+} ions (at 1 mol% of Nd_2O_3) in the barium ferrite lattice could produce a significant change in the crystal structure as verified by the XRD pattern of NdBF1. The emergence of two new peaks in NdBF1 corresponding to a primary phase of $Ba_6Nd_2Fe_4O_{15}$ and a secondary phase of $BaFe_{18}O_{27}$ were clearly disclosed. The occurrences of sharp XRD peaks were allotted to the hexagonal lattice of $Ba_6Nd_2Fe_4O_{15}$ (matched with the ICDD number 01-079-2141) with $a = b = 1.1815$ nm, $c = 0.7078$ nm, $\alpha = \beta = 90°$ and $\gamma = 120°$. Moreover, the peak centered at 32.17° was endorsed to the hexagonal crystalline lattice of $BaFe_{18}O_{27}$ (matched with the ICDD number 01-075-0406). The inclusion of 2 mol% of Nd_2O_3 (sample NdBF2) into the BFCs could transform the crystalline phase from hexagonal $BaFe_{18}O_{27}$ to orthorhombic $BaFe_2O_4$ structure (matched with the ICDD number 01-077-2337). Meanwhile, further addition of Nd_2O_3 up to 3 mol% in the BFCs (sample NdBF3) led to an alteration in the XRD peak position of $BaFe_2O_4$ without significant variations in the phase and structure. It was affirmed that the replacement of Fe^{3+} by Nd^{3+} ions in the studied BFCs could generate a new primary hexagonal crystalline phase of $Ba_6Nd_2Fe_4O_{15}$. Widening of the diffraction peaks for all as-synthesized NdBFCs is credited to the nano-crystalline size and lattice strain.[24,25] The crystallite sizes of the studied $Ba_6Nd_2Fe_4O_{15}$ (calculated using the Debye-Scherrer's equation) were ranged from 15 to 67 nm.

3.3. Magnetic properties

Fig. 4 depicts the magnetization (M) concerning the applied field (H) of all the studied barium ferrites without and with Nd^{3+} ions substitution. The composite without containing Nd^{3+} ions (NdBF0) revealed that the saturation magnetization (M_s), remanence magnetization (M_r), and coercivity field (H_c) were 16.36 emu/g, 11.82 emu/g and 0.24 T, respectively. The overall magnetic behavior of the composite (NdBF1), except for the M_s did not significantly change due to addition of 1 mol% of Nd_2O_3. The inclusion of 2 mol% Nd_2O_3 into the composite (NdBF2) did not affect the value of M_s. However, incorporation of 3 mol% Nd_2O_3 into the composite (NdBF3) could lead to an increase in the value of M_s comparable to NdBF1, which was ascribed to the enhanced porosity of the barium ferrite surface. It was argued that the occurrence of such excessive porosity could isolate the magnetic domain walls, leading to natural polarization of the unpaired magnetic spins in the presence of an externally applied magnetic field. The magnetic hysteresis loop of NdBF0 coincided with NdBF2. Similarly, the magnetic hysteresis loop of NdBF1 was overlapped with NdBF3. Thus, it was established

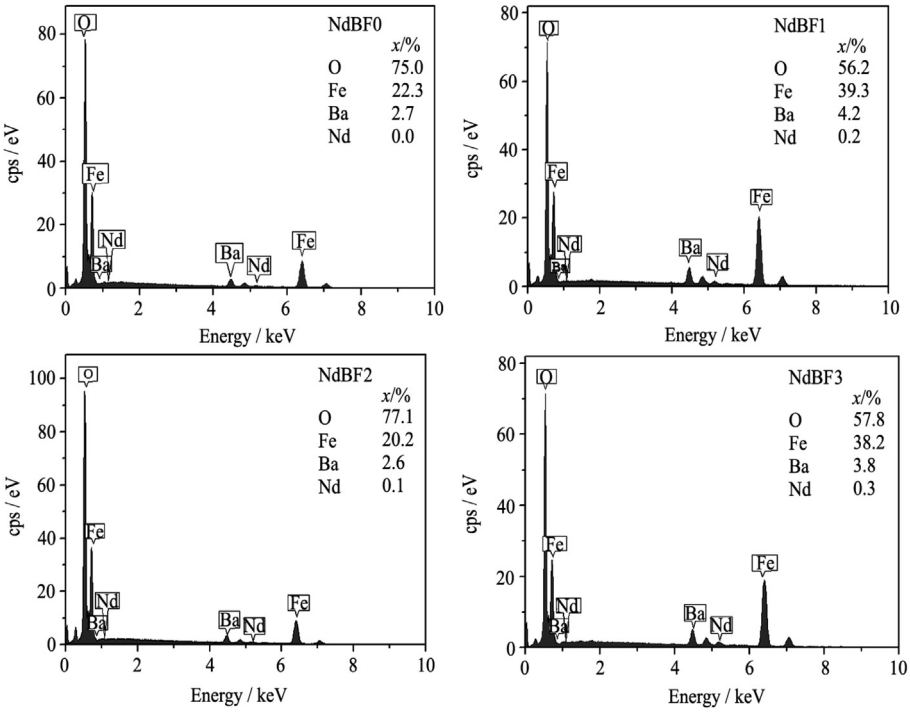

Fig. 2. EDX spectra of the as-synthesized NdBFCs.

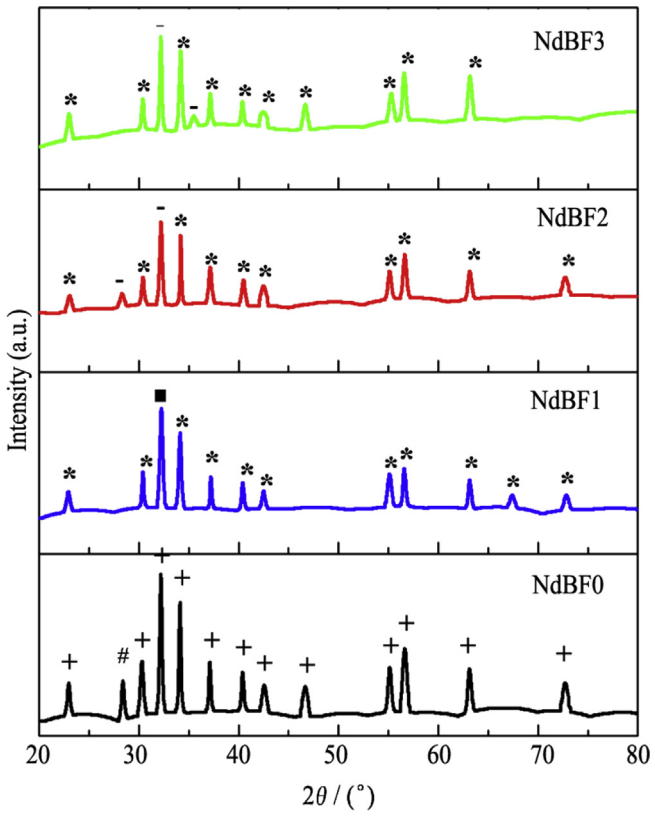

Fig. 3. XRD patterns of all as-synthesized NdBFCs. * $Ba_6Nd_2Fe_4O_{15}$; + $BaFe_{12}O_{19}$; ■ $BaFe_{18}O_{27}$; – $BaFe_2O_4$; # $Fe_{21.333}O_{32}$.

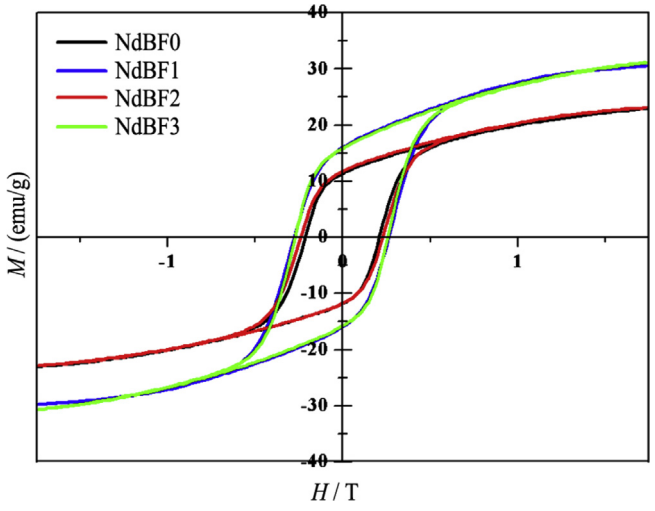

Fig. 4. Hysteresis loops of the studied NdBFCs

that such pair ferrites (NdBF0 and NdBF2 as well as NdBF1 and NdBF3) had almost identical magnetic properties. Disclosure of such narrow hysteresis loops (loop-gap area) indeed confirmed the soft magnetic character of the proposed BFCs. On top, the studied composites failed to display the complete saturation magnetization because of the presence of antimagnetic materials such as $BaFe_2O_4$ and $Fe_{21.333}O_{32}$. The underlying development of the non-magnetic phase because of a sintering procedure at high temperature is likewise in charge of altering M_s.[25,26]

3.4. Complex relative permittivity and permeability

Fig. 5(a) shows the frequency-dependent complex relative permittivity (ε_r) for all composites in the X-band. The real (ε') and imaginary (ε'') components of the permittivity of the prepared composites aroused from the intrinsic electric dipole polarization strongly depended on the MW frequencies.[27] Actually, the real part of the permittivity signified the energy stored in the material from an external electric field.[28] The real part of the permittivity revealed three prominent resonance peaks around 8.7, 10.0 and 11.8 GHz, indicating the storage of energy in the composites from the electric field. Nevertheless, the lack of stored energy could be observed at other MW frequencies. Meanwhile, the imaginary part of the permittivity signified the dielectric loss factor, denoting the energy dissipation capacity of the material. The appearance of the resonance peaks in the ε' spectrum was trailed by the disappearance of the resonance peaks in the ε'' spectra.[13] It was affirmed that the proposed composites presented the best energy storage performance around 11.6 GHz, wherein the absorbed energy was consumed for the magnetic domain wall motion.

Fig. 5(b) illustrates the frequency dependent complex relative permeability for all composites in the X-band. The real part of the permeability (μ') exhibited three significant resonance peaks around 8.5, 9.3 and 11.0 GHz, demonstrating the magnetic energy storage capacity of the composites. Alternatively, the imaginary part of the permeability (μ'') revealed the magnetic loss factor around 8.2, 9.0, and 10.5 GHz, which was allocated to the natural resonance frequency f_r.[13] Besides, the magnetic loss factor was increased at the resonance frequency. It was observed that the substitution of Fe^{3+} in the BFCs by Nd^{3+} at varied concentrations caused the frequency shift. This disclosure was attributed to the emergence of different phases and porosity in the composites. The imaginary part of the permeability plays an important role in the microwave absorbing property of hexaferrites[29] that are related to the relaxation of domain wall resonance.[30]

3.5. Microwave reflection loss

Fig. 6 represents the variation in the reflection loss (R_L) of all prepared BFCs as a function of applied MW frequency (f). The NdBF0 and NdBF3 composites revealed a similar trend in the R_L pattern which comprised of two weak absorption bands with values above −10 dB. Meanwhile, the NdBF1 specimen exhibited R_L value below −10 dB at frequencies range of 9.14–10.18 GHz. Besides, NdBF2 composite disclosed two prominent absorption bands centered around 9.94 and 11.64 GHz with R_L values of −22.94 and −23.82 dB, respectively. All the observed spectral bands showed a significant shift with varying contents of Nd^{3+} ions with the bandwidth of less than 1 dB. In short, the microwave absorption capacity of the proposed BFCs was improved due to Nd^{3+} ions substitution assisted enhanced porosity in the structure that in turn could confine the MW. Consequently, the Nd^{3+} ions substitution into the BFs could change the magnetocrystalline anisotropy direction of the composites, leading to an alteration of the natural resonance frequency. This alteration could finally cause a shift of the MW reflection loss to high-frequency zone as revealed by NdBF2. Interestingly enough, the doped composites enriched in $Ba_6Nd_2Fe_4O_{15}$ and $BaFe_2O_4$ phases could absorb microwaves selectively in the X-band.

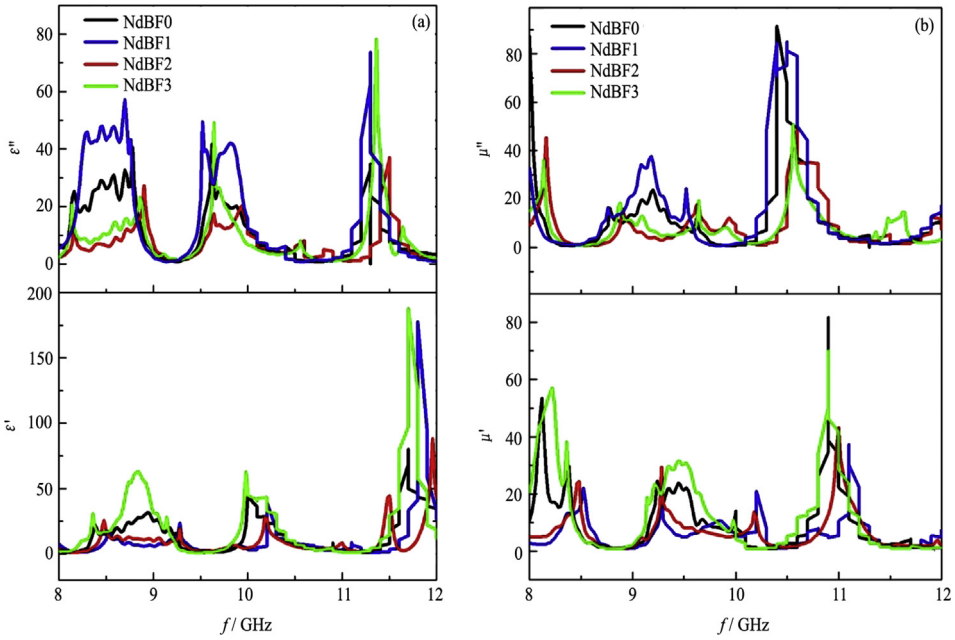

Fig. 5. Frequency-dependent complex relative permittivity (a) and permeability (b) for all NdBFCs.

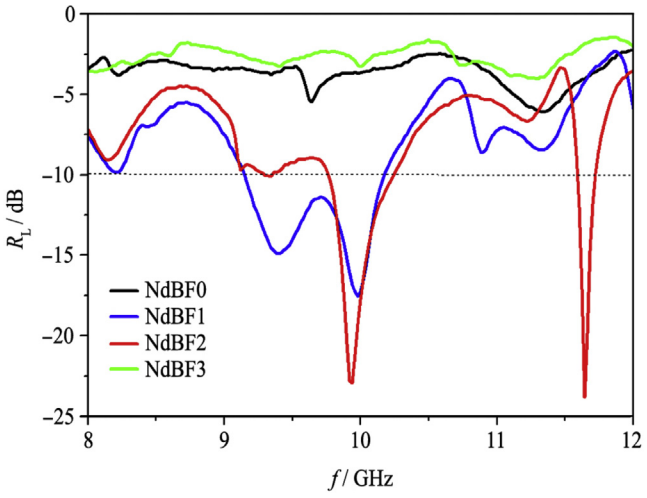

Fig. 6. Frequency-dependent MW reflection loss of all the proposed NdBFCs

4. Conclusions

Synthesis and room temperature characterization of some new hexagonal barium ferrite composites with Nd^{3+} ions substitution were reported. An appropriate amount of chemical constituents were gradually mixed to prepare these composites following solid-state reaction route. The proposed BFCs reveal excellent capacity of MW absorption in the X-band. EDX spectra reveal the right elemental compositions of the prepared BFCs and presence of Nd in the structures. The surface morphology, structure, magnetic properties and MW absorption ability of the prepared BFCs are strongly influenced because of the inclusion of Nd^{3+} ions into the crystalline lattice. The XRD pattern discloses the formation of new crystalline phases of $Ba_6Nd_2Fe_4O_{15}$ and $BaFe_2O_4$ due to the incorporation of Nd^{3+} ions into the BFCs structure. SEM images of the studied BFCs exhibit highly rough and porous surface morphology. At 2 mol% of Nd^{3+} ions, the saturation magnetization of the BFCs displays insignificant alteration. The complex relative permittivity and permeability of the studied BFCs are found to depend appreciably on the MW frequencies. Furthermore, the achieved low reflection loss at 9.94 and 11.64 GHz frequencies with selective MW absorption shown by the proposed BFCs may be advantageous for diverse device applications in the X-band.

Acknowledgments

Authors are grateful to Universitas Jenderal Soedirman, Kemenristekdikti Indonesia, and UTM Malaysia for financial assistance.

References

1. Kim MS, Koh JG. Microwave-absorbing characteristics of NiCoZn ferrite prepared by using a co-precipitation method. *J Korean Phys Soc*. 2008;53:737.
2. Yuan CL, Tuo YS. Microwave adsorption of $Sr(MnTi)_xFe_{12-2x}O_{19}$ particles. *J Magn Magn Mater*. 2013;342:47.
3. Sun C, Sun KN, Chui PF. Microwave absorption properties of Ce-substituted M-type barium ferrite. *J Magn Magn Mater*. 2012;324:802.
4. Dong CS, Wang X, Zhou PH, Liu T, Xie JL, Deng LJ. Microwave magnetic and absorption properties of M-type ferrite $BaCo_xTi_xFe_{12-2x}O_{19}$ in the Ka band. *J Magn Magn Mater*. 2014;354:340.
5. Salman S, Afghahi SSS, Jafarian M, Atassi Y. Microstructural and magnetic studies on $BaMg_xZn_xX_{2x}Fe_{12-4x}O_{19}$ (X=Zr,Ce,Sn) prepared via mechanical activation method to act as a microwave absorber in X-band. *J Magn Magn Mater*. 2016;406:184.
6. Qiao ZQ, Pan SK, Xiong JL, Cheng LC, Yao QR, Lin PH. Magnetic and microwave absorption properties of La-Nd-Fe alloys. *J Magn Magn Mater*. 2017;423:197.
7. Taurino R, Karamanov A, Rosa R, Karamanova E, Barbieri L, Atanasova-Vladimirova S. New ceramic materials from MSWI bottom ash obtained by an innovative microwave-assisted sintering process. *J Eur Ceram Soc*. 2017;37:323.
8. Liu G, Wang LY, Yang ZH, Wu RB. Synthesis of iron-based hexagonal microflakes for strong microwave attenuation. *J Alloys Compd*. 2017;718:46.
9. Bibi M, Abbas SM, Ahmad N, Muhammad B, Iqbal Z, Rana UA. Microwaves absorbing characteristics of metal ferrite/multiwall carbon nanotubes nanocomposites in X-band. *Compos B Eng*. 2017;114:139.
10. Luo JL, Pan SK, Cheng LC, Lin PH, He Y, Chang JQ. Electromagnetic and microwave absorption properties of Er-Ho-Fe alloys Jialiang. *J Rare Earths*. 2018;36:715.
11. Liu Y, Wang TJ, Liu Y, Li XJ, Liu Y. Mechanism for synthesizing barium hexagonal ferrite by sol-gel method. *Adv Mater Res*. 2012;549:105.
12. Bierlich S, Gellersen F, Jacob A, Töpfer J. Low-temperature sintering and magnetic properties of Sc- and In-substituted M-type hexagonal barium ferrites for microwave applications. *Mater Res Bull*. 2017;86:19.

13. Widanarto W, Amirudin F, Ghoshal SK, Effendi M, Cahyanto WT. Structural and magnetic properties of La^{3+} substituted barium–natural nanoferrites as microwave absorber in X-band. *J Magn Magn Mater*. 2017;426:483.
14. Kanna RR, Lenin N, Sakthipandi K, Sivabharathy M. Impact of lanthanum on structural, optical, dielectric and magnetic properties of $Mn_{1-x}Cu_xFe_{1.85}La_{0.15}O_4$ spinel nanoferrites. *Ceram Int*. 2017;43:15868.
15. Bhongale SR, Ingawale HR, Shinde TJ, Vasambekar PN. Effect of Nd^{3+} substitution on structural and magnetic properties of mg-cd ferrites synthesized by microwave sintering technique. *J Rare Earths*. 2018;36:390.
16. Ahmed MA, Okasha N, Kershi RM. Influence of rare-earth ions on the structure and magnetic properties of barium W-type hexaferrite. *J Magn Magn Mater*. 2008;320:1146.
17. Shen GZ, Xu Z, Li Y. Absorbing properties and structural design of microwave absorbers based on W-type La-doped ferrite and carbon fiber composites. *J Magn Magn Mater*. 2006;301:325.
18. Wang J, Zhang H, Bai SX, Chen K, Zhang CR. Microwave absorbing properties of rare-earth elements substituted W-type barium ferrite. *J Magn Magn Mater*. 2007;312:310.
19. Deng LW, Ding L, Zhao KS, Huang SX, Hu ZW, Yang BC. Electromagnetic properties and microwave absorption of W-type hexagonal ferrites doped with La^{3+}. *J Magn Magn Mater*. 2011;323:1895.
20. Seyyed Afghahi SS, Jafarian M, Salehi M, Atassi Y. Improvement of the performance of microwaveX band absorbers based on pure and doped Ba-hexaferrite. *J Magn Magn Mater*. 2017;421:340.
21. Widanarto W, Ardenti E, Ghoshal SK, Kurniawan C, Effendi M, Cahyanto WT. Significant reduction of saturation magnetization and microwave-reflection loss in barium-natural ferrite via Nd^{3+} substitution. *J Magn Magn Mater*. 2018;456:288.
22. Widanarto W, Jandra M, Ghoshal SK, Effendi M, Cahyanto WT. $BaCO_3$ mediated modifications in structural and magnetic properties of natural nanoferrites. *J Phys Chem Solids*. 2015;79:78.
23. Widanarto W, Rahayu FM, Ghoshal SK, Effendi M, Cahyanto WT. Impact of ZnO substitution on magnetic response and microwave absorption capability of strontium-natural nanoferrites. *Results Phys*. 2015;5:253.
24. Vinila VS, Jacob R, Mony A, Nair HG, Issac S, Rajan S, et al. XRD studies on nano crystalline ceramic superconductor PbSrCaCuO at different treating temperatures. *Cryst Struct Theor Appl*. 2014;3:1.
25. Dabagh S, Ati AA, Rosnan RM, Zare S, Othaman Z. Effect of Cu-Al substitution on the structural and magnetic properties of Co ferrites. *Mater Sci Semicond Process*. 2015;33:1.
26. Ewais EMM, Hessien MM, El-Geassy A-HA. *In-situ* synthesis of magnetic Mn-Zn ferrite ceramic object by solid state reaction. *J Australas Ceram Soc*. 2008;44:57.
27. Wang L, Yu HT, Ren XH, Xu GL. Magnetic and microwave absorption properties of $BaMn_xCo_{1-x}TiFe_{10}O_{19}$. *J Alloys Compd*. 2014;588:212.
28. Das CK, Bhattacharya P, Kalra SS. Graphene and MWCNT: potential candidate for microwave absorbing materials. *J Mater Sci Res*. 2012;1:126.
29. Wang LX, Huang Q, Mu L, Zhang QT. Influence of Sm^{3+} substitution on microwave magnetic performance of barium hexaferrites. *J Rare Earths*. 2007;25:216.
30. Wang L, Lin PH, Pan SK, Zhou HY. Microwave absorbing properties of NdFeCo magnetic powder. *J Rare Earths*. 2012;30:529.